Membrane Currents in Taste Cells of the Rat Fungiform Papilla

Evidence for Two Types of Ca Currents and Inhibition of K Currents by Saccharin

PHILIPPE BÉHÉ, JOHN A. DESIMONE, PATRICK AVENET, and BERND LINDEMANN

From the Department of Physiology, Universität des Saarlandes, D-6650 Homburg/Saar, Federal Republic of Germany

ABSTRACT Taste buds were isolated from the fungiform papilla of the rat tongue and the receptor cells (TRCs) were patch clamped. Seals were obtained on the basolateral membrane of 281 TRCs, protruding from the intact taste buds or isolated by micro-dissection. In whole-cell configuration 72% of the cells had a TTX blockable transient Na inward current (mean peak amplitude 0.74 nA). All cells had outward K currents. Their activation was slower than for the Na current and a slow inactivation was also noticeable. The K currents were blocked by tetraethylammonium, Ba, and 4-aminopyridine, and were absent when the pipette contained Cs instead of K. With 100 mM Ba or 100 mM Ca in the bath, two types of inward current were observed. An L-type Ca current ($I\mathrm{Ca_L}$) activated at -20 mV had a mean peak amplitude of 440 pA and inactivated very slowly. At 3 mM Ca the activation threshold of $I\mathrm{Ca_L}$ was near -40 mV. A transient T-type current ($I\mathrm{Ca_T}$) activated at -50 mV had an average peak amplitude of 53 pA and inactivated with a time constant of 36 ms at -30 mV. $I\mathrm{Ca_L}$ was blocked more efficiently by Cd and D600 than $I\mathrm{Ca_T}$. $I\mathrm{Ca_T}$ was blocked by 0.2 mM Ni and half blocked by 200 μM amiloride. In whole-cell voltage clamp, Na-saccharin caused (in 34% of 55 cells tested) a decrease in outward K currents by 21%, which may be expected to depolarize the TRCs. Also, Na-saccharin caused some taste cells to fire action potentials (on-cell, 7 out of 24 cells; whole-cell, 2 out of 38 cells responding to saccharin) of amplitudes sufficient to activate $I\mathrm{Ca_L}$. Thus the action potentials will cause Ca inflow, which may trigger release of transmitter.

Address reprint requests to Dr. B. Lindemann, Department of Physiology, Universität des Saarlandes, D-6650 Homburg/Saar, FRG.

Dr. DeSimone's permanent address is Department of Physiology, Virginia Commonwealth University.

J. GEN. PHYSIOL. © The Rockefeller University Press · 0022-1295/90/11/1061/24 $2.00 1061
Volume 96 November 1990 1061–1084

INTRODUCTION

Recent electrophysiological investigations, including patch clamp experiments, have shown that amphibian taste receptor cells (TRCs) are able to generate action potentials in response to electrical stimulation (Roper, 1983; Kashiwayanagi et al., 1983; Avenet and Lindemann, 1987*a*, *b*; Kinnamon and Roper, 1987; Miyamoto et al., 1988; Teeter et al., 1989). Action potentials were also observed in response to tastants like acid (Kinnamon and Roper, 1988) or salt (Avenet and Lindemann, 1987a). Furthermore, Ca currents were demonstrated, suggesting that Ca inflow mediates transmitter release (Kinnamon and Roper, 1988; Teeter et al., 1989). It seems, therefore, that voltage-gated Na and Ca conductances play an important role in the amphibian TRCs.

The case is less clear for mammalian TRCs. Available data are restricted to cells from the circumvallate papilla. One study concerned with the bitter response describes only a few cells with transient Na inward currents (Akabas et al., 1988, 1990). Denatonium, a strong bitter tastant, caused release of Ca from intracellular stores. No plasma membrane Ca currents were required. In another study, also concerned with the bitter response in mice, half of the cells investigated had voltage-gated Na currents (Spielman et al., 1989) and denatonium decreased outward K currents.

In this study we were mainly interested in the response to "sweet." A method to patch clamp TRCs from the rat fungiform papilla was developed. We report that voltage-gated Na and Ca conductances are present in most of the TRCs and that action potentials can occur in response to sweet stimulation. According to the thresholds estimated, the action potentials will trigger inflow of Ca (which probably mediates release of transmitter). Part of our results appeared in preliminary form (Béhé et al., 1989*a*).

MATERIALS AND METHODS

Isolation of the Taste Cell

Female Wistar rats weighing ~250 g were killed by dislocation of the cervical vertebrae. The tongue was rapidly removed and stored for no longer than 5 min in an ice-cold Tyrode solution pre-equilibrated with 100% O_2.

A high K culture medium solution (KCM) containing 4 mg/ml collagenase and 2 mg/ml trypsin inhibitor was injected into the tongue (0.5–1 ml/tongue) from the cut end with a thin needle. The tip of the needle was carefully pushed through the superficial parts of tongue muscle as close as possible to the epithelium. Due to the injected volume the tongue was slightly swollen. A small hook was attached to the cut end and the tongue was suspended at room temperature in a 50-ml beaker containing a 0 mM Ca, 2 mM EGTA Tyrode solution equilibrated with 100% O_2. During the incubation care was taken to avoid any contact of the external tongue surface with small amounts of collagenase solution leaking out of the injection puncture.

After 30 min the epithelium containing the taste buds could be gently pealed off from the underlying muscle. It was then rinsed and placed upside-down under a binocular dissecting microscope of 10–40× magnification. In this condition the taste buds (40 μm in diameter) could be seen inside the fungiform papillae (one taste bud per papilla). A glass capillary with an opening of ~50 μm was introduced in the papillae and the taste buds were individually

sucked into the capillary. This was possible because the external low Ca treatment, concomitant with the internal collagenase treatment, had loosened the tight junctions and therefore the attachment of the buds to the papillae. In some cases the attachment was too strong and a complementary 0-mM Ca treatment of 10–20 min was necessary.

The taste buds were allowed to settle in Tyrode solution on the bottom of a chamber that consisted of a standard glass slide onto which a silicon ring of 1-mm thickness and 10-mm inner diameter was pressed. The bottom of the chamber was covered with a thin layer of Cell-Tak (1 $\mu g/cm^2$; Bio-Polymers, Inc., Farmington, CT) before use. After attachment of the buds the Tyrode solution was replaced by the KCM solution and the chamber was stored on ice in a 100% O_2 atmosphere until use.

For patch clamping, the chamber was placed on the stage of an inverted microscope (model IMT2-F; Olympus Corporation of America, New Hyde Park, NY) and the cells were superfused at ~0.5 ml/min with appropriate solutions at room temperature. The cells were viewed with Nomarski optics at a total magnification of 400×.

Electrical Recordings

The procedure for whole-cell recording closely followed the description by Hamill et al. (1981). Patch pipettes were pulled from thick-walled borosilicate glass capillaries (outer diameter 2 mm, inner diameter 1–1.25 mm; Jencons Scientific Ltd., Bedfordshire, UK) on a two-stage puller designed in the laboratory. After fire-polishing, the tip resistances were 7–10 MΩ when filled with Tyrode solution.

The pipettes were manipulated with a hydraulic 3-D manipulator (model MO-103N-L; Narishige Scientific Laboratory, Tokyo, Japan). Patch-clamp currents were recorded with the EPC-7 amplifier (List Electronic, Darmstadt, FRG). Current and voltage signals were digitized at 40 kHz (16 bits) with an audio-PCM processor (model 501 ES, modified to pass zero frequency; Sony) and stored on a video tape recorder. Current and voltage pulses could also be simultaneously digitized with an analog-to-digital converter (DASH-16; Metrabyte, Taunton, MA) with a sample rate up to 30 kHz and stored on the disk of an IBM AT computer. A program written in the laboratory allowed for the construction of the current–voltage diagrams.

Solutions and Reagents

The high KCM, prepared in the laboratory, contained (in mM): 103 KCl, 0.42 $Ca(NO_3)_2$-$4H_2O$, 0.41 $MgSO_4$-$7H_2O$, 8.43 Na_2HPO_4-$2H_2O$, 10 D-glucose, 25.2 HEPES (pH 7.4), and phenol red (5 mg/ml). Basal medium Eagle amino acids (100×) and vitamins (100×), MEM nonessential amino acid (100×) (all from Gibco Laboratories, Grand Island, NY), penicillin/streptomycin (10,000 E/10,000 μg per ml) (Seromed, Berlin, FRG) were each added at 1% and fetal calf serum (Seromed) was added at 10%. The Tyrode solution contained (in mM): 140 NaCl, 5 KCl, 1 $MgCl_2$, 1 $CaCl_2$, 10 HEPES (pH 7.4), 10 glucose, and 10 pyruvate. The standard pipette filling solution for whole-cell recording contained (in mM): 140 KCl, 2 $MgCl_2$, 1 $CaCl_2$, 11 EGTA (pCa 8), 10 HEPES-KOH (pH 7.2), and 5 ATP.

Nystatin (Sigma Chemical Co., St. Louis, MO) was first dissolved in DMSO under strong stirring to give a stock solution of 50 mg/ml, which was prepared new for each experiment. The stock nystatin was added to the pipette solution to give a final concentration of 300 μg/ml and the solution was sonicated before each use.

The following chemicals were used in addition: Cell-Tak, concanavalin A (type IV; Sigma Chemical Co.), poly-L-lysine (Sigma Chemical Co.), collagenase (type A; Boehringer Mannheim Biochemicals, Indianapolis, IN), trypsin inhibitor (type I; Sigma Chemical Co.), tetrodotoxin (TTX; Sigma Chemical Co.), tetraethylammonium (TEA; Sigma Chemical Co.), 4-amino-

pyridine (4AP; E.G.A., Steinheim, FRG), D-600 (Knoll A.G., Ludwigshafen, FRG), amiloride (Sharp & Dohme GmbH, Munich, FRG), ATP (di-Na salt; Sigma Chemical Co.), adenosine 3′5′-cyclic monophosphate (cAMP; Serva Fine Biochemicals Inc., Garden City Park, NY), 8-bromoadenosine 3′5′-cyclic monophosphate (8-Br cAMP; Sigma Chemical Co.), dibutyryl adenosine 3′5′-cyclicmonophosphate (di-but-cAMP; Sigma Chemical Co.), chlorophenylthio-adenosine 3′5′-cyclic monophosphate (cpt-cAMP; Sigma Chemical Co.), 3-isobutyl-l-methyl-xanthine (IBMX; Sigma Chemical Co.).

Means are given ± standard deviation with the number of observations (n) in parentheses.

RESULTS

Taste Cell Preparation

The onion-shaped taste bud of the rat, 30–50 μm in diameter, contains 50–100 cells, 50–70% of which are TRCs (Farbman, 1965; Murray, 1971). We developed a protocol that allowed the buds to retain their shape when isolated from the tongue epithelium. The spindle shape of the TRCs and their orientation within the bud were also preserved. Typically the TRCs converged at the apical pole (Fig. 1, *A–C*), as also seen in microscopic sections (Farbman, 1965). The main feature of the protocol is the use of the high KCM. When Tyrode or Na culture medium was used instead of the KCM to prepare the buds, or when the collegenase treatment was prolonged, the buds had a more globular shape and more lysed cells were observed at their periphery. The best results were obtained when the isolation protocol was as short as possible, i.e., when the buds were patch clamped 45 min after the death of the rat.

To allow superfusion with saline, the buds were attached to the bottom of the experimental chamber. This was achieved by covering the glass bottom with concanavalin A, poly-L-lysine, or Cell-Tak. We preferred Cell-Tak because concanavalin was reported to affect Ca currents (Ivens and Deitmer, 1986) and poly-L-lysine can cause a nonspecific increase in membrane conductance (Hammes and Schullery, 1970).

To gain access to taste cells located within the bud, a further dissection was done under the microscope. With the buds strongly attached to the dish, taste cells could be pulled off, one by one, with a patch pipette (Fig.1., *D* and *E*). Seals were easily obtained, either on cells from the periphery of the intact taste buds or on single cells isolated by micro-dissection. We recorded from 281 cells.

On-Cell Recordings

In the process of sealing, TRCs often generated action potentials, probably caused by depolarization due to mechanical disturbance. The action potentials became noticeable as fast, biphasic current transients, as observed in other excitable cells (Fenwick et al., 1982*a;* Rorsman and Trube, 1986). The transients consisted of conductive and capacitance currents driven by the cellular voltage change. Action potentials were also generated in response to electrical stimulation. It appears that the patch was sufficiently leaky and the cell resistance sufficiently large for a current of 3 pA to depolarize the membrane potential to threshold. Fig. 2 *A* shows current traces obtained by step depolarizing the pipette interior from a −80-mV holding voltage. The short transients are indicative of action potentials. The stronger the

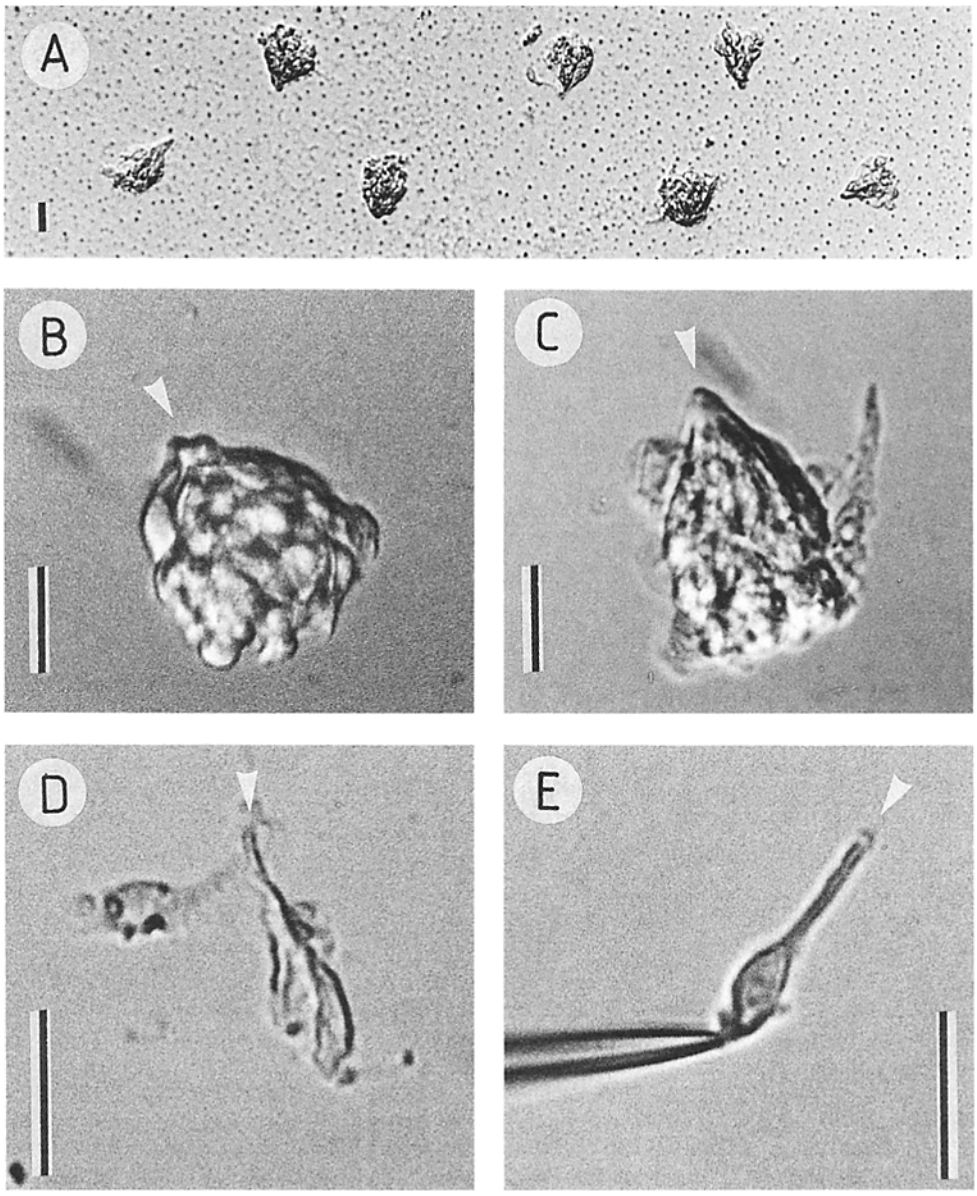

FIGURE 1. Taste buds and taste cells isolated from the rat fungiform papilla. *A*, Low magnification view of the experimental chamber containing several taste buds. *B* and *C*, Single taste buds seen at higher magnification. Note the convergence of the taste cells at the apical pole (*arrows*). *C* contains some lysed cells at the periphery of the bud. *D* and *E*, Taste cells isolated by dissecting the buds under the microscope. A single taste cell was patched in *E*. The arrows indicate the apical pole of the cell. All bars, 20 μm.

depolarization, the shorter the interval between the spikes. A graded decrease of the spike amplitude occurred within each group.

Two types of current transients were observed. Type I transients were biphasic, almost symmetrical (Fig. 2 *B*). They are mainly derivatives of action potentials, which have comparable rates of depolarization (positive phase) and repolarization (negative phase of the current transient). Type II transients (Fig.2 *C*) were strongly asymmetrical, the negative phase being very small. Because the time course of the positive phase of both types could be superimposed, we attribute the small negative phase in type II to a slow repolarization of the action potential rather than to an increased

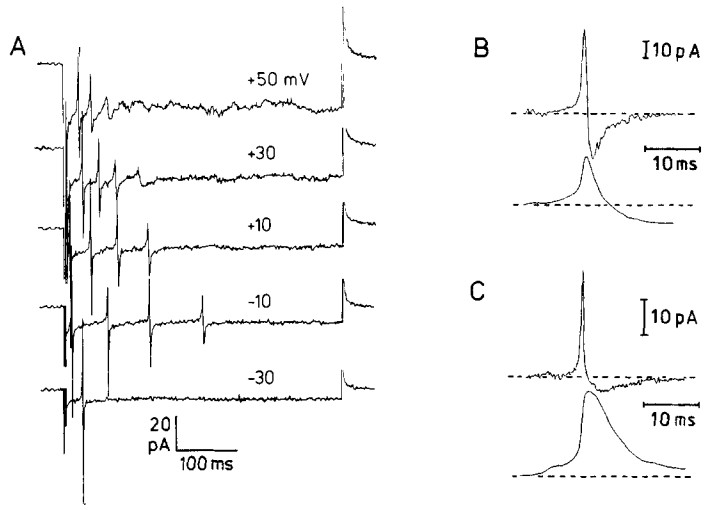

FIGURE 2. On-cell recording of current transients driven by cellular action potentials. *A*, Starting from the pipette holding voltage of −80 mV, step command pulses (millivolt values indicated) were applied which depolarized the cell. A 3-pA current was sufficient to trigger an action potential (lower current time course). For clarity, curves were displaced horizontally for an arbitrary distance. *B* and *C*, Current transients driven by spontaneous action potentials (upper traces) and corresponding computer integration (lower traces). Type I transient (*B*) was symmetrical and its integration yielded to an action potential–like time course having a fast falling phase. Type II transient (*C*) had a smaller negative-oriented phase which produced a slower repolarization in the integrated trace. For *A*, *B*, and *C* the pipette contained the standard KCl filling solution and the bath solution was Tyrode.

conductive current component. However, a conductive component may also contribute to the current transient. The integration of the digitized trace of the current transients (Fig. 2, *B* and *C*) resembled the action potentials measured in whole-cell current clamp (Fig. 3). A marked after-hyperpolarization, often seen on the integrated traces, was probably due to asymmetrical conductive current flowing through the patch. The current transients were not affected by the Ca channel blockers Cd and Ni (see below).

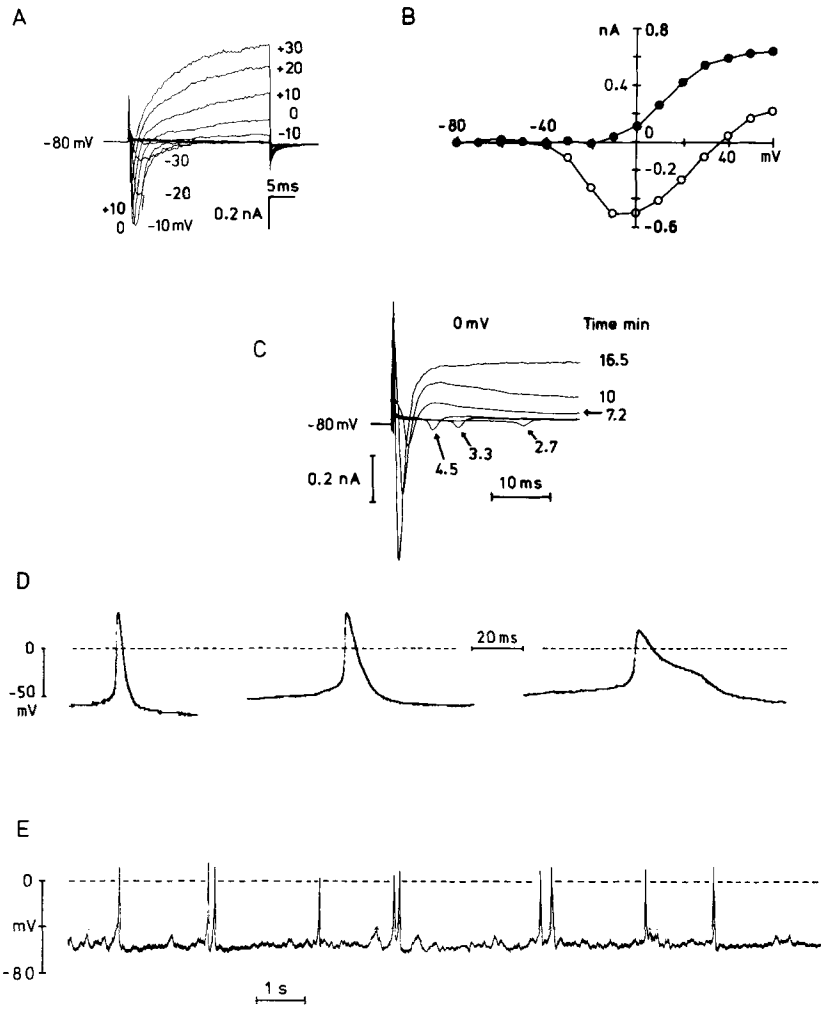

FIGURE 3. Whole-cell recordings from TRCs. *A*, Current time courses in response to depolarizations from a −80-mV holding voltage to the values indicated. The patch was broken with a suction pulse. *B*, Corresponding maximum inward and outward currents plotted against the command pulse voltage. *C*, Progressive permeabilization of the membrane patch as a result of the nystatin channel incorporation. The current time courses in response to a voltage pulse from −80 to 0 mV, recorded at the time indicated after sealing, were superimposed. Capacitive currents were not compensated. Before the backloading of the pipette with the nystatin-containing solution (300 μg/ml), the tip was filled with the standard KCl pipette solution. *D* and *E*, Whole-cell current-clamp recordings of spontaneous action potentials in three different cells. *D*, Type I action potential with a fast repolarizing phase (*left*), type II action potential with a longer repolarizing phase (*middle*), and action potential having a shoulder on the repolarizing phase (*right*). *E*, Same TRC as in *D* (*right*) at a compressed time scale. The pipette contained the standard KCl filling solution and the bath was Tyrode.

Whole-Cell Recordings

To obtain the whole-cell recording configuration, the patch was broken with a suction pulse. When the pipette contained KCl and the bath Tyrode, the cells had an input slope resistance of 1–3 GΩ, a membrane capacitance of 3–5 pF, and a zero current potential ranging between −70 and −50 mV when stable. Step-depolarizations from −80 mV resulted in the current time courses of Fig. 3 *A*. In 204 of 281 cells (72%) as fast transient inward current was elicited when the voltage exceeded −50 mV, and was followed by a more slowly developing outward current. The remaining 77 cells showed only outward currents. The inward current was blocked by 2 μM TTX and disappeared when *N*-methyl-D-glucamine (NMDG) replaced Na. The outward current vanished when CsCl or NMDG replaced KCl in the pipette filling solution (Fig. 4 *A*). These results, as well as the current–voltage relationships for the peak and steady-state currents (Fig. 3 *B*), suggest that the rat TRCs have the classical voltage-gated Na and K currents of excitable cells.

To avoid the dialysis of cellular constituents and to preserve the natural intracellular Ca concentration, we used the "nystatin-perforated patch method" described by Horn and Marty (1988). The tip of the pipette was filled with normal pipette solution and the solution containing nystatin (300 μg/ml) was backloaded. The incorporation of the nystatin channel in the patches could be followed by monitoring the changes in the biphasic current transients elicited by a constant depolarizing pulse. The delay of the current transient progressively decreased (Fig. 3 *C*) and its amplitude increased. Within 20 min the time course of the inward current progressively turned from an extracellularly measured capacitive transient (cell unclamped) to a typical whole-cell clamp current. The only difference in the membrane current properties, when this method was used instead of the mechanical break-through, was a shift in the activation of the Na current (see below).

Whatever the method used to obtain the whole-cell configuration, stable current clamp conditions were rarely obtained. Many cells depolarized within 1–3 min after opening the patch. This might be due to the high input slope resistance of the TRCs, a small current change affecting strongly the resting voltage. In cases where a stable potential was recorded for a longer period, the cells sometimes fired spontaneous action potentials (Fig. 3, *D* and *E*). As found with the on-cell mode, the action potentials were of two types. Type I has a fast rising and a fast falling phase and resembled the integrated current trace of Fig. 2 *B*. Type II had a slower falling phase and resembled the integrated current of Fig. 2 *C*. In only a few cases the action potentials had a shoulder or a very slow repolarizing phase, lasting up to 30 ms (Fig. 3 *D*, right-most curve).

Voltage-gated Inward Na Current

Thresholds for Na current activation ranged from −60 to −50 mV. The peak amplitude, reached between −30 and −10 mV, averaged 0.74 ± 0.67 (76) nA. Kinetic parameters were studied when the KCl of the pipette solution was replaced by CsCl or NMDG to eliminate the outward currents (Fig. 4, *A* and *B*). The time to peak was 0.13 ms for a −30-mV depolarizing pulse, and at the same voltage the inactivation time course, approximated with a single exponential, had a time

constant of 3 ms. When the cells were dialyzed with CsCl and NMDG, or when the patches were permeabilized with nystatin, thresholds tended to be more negative, activation was steeper, and a delay in the current development was often observed. These effects were probably due to a remaining series resistance causing the cell

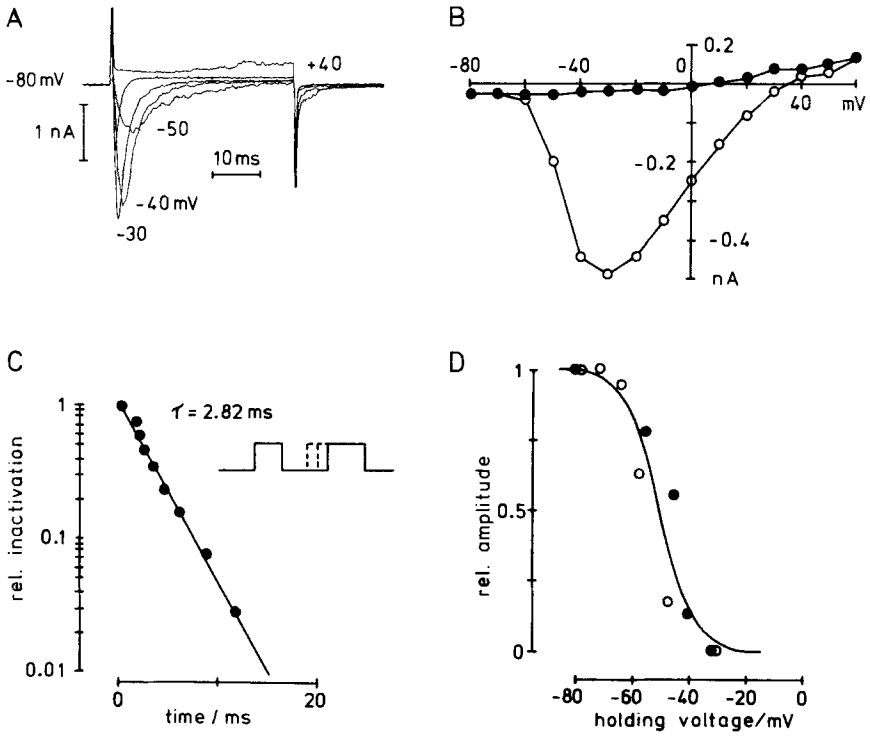

FIGURE 4. The transient Na-inward current. *A*, Current time courses in response to depolarizations, at the voltage indicated, from a −80-mV holding voltage. The K of the standard pipette solution was replaced by NMDG and the bath was Tyrode. *B*, Peak currents (*open circles*) and steady-state currents (*solid circles*), obtained under the conditions of *A*, as a function of pulse voltage. A steady-state leakage current of 10–50 pA was always observed. *C*, The recovery at −80 mV of the Na current inactivation was evaluated with two pulses (prepulse and test pulse) applied at variable intervals. The relative inactivation was measured as $1-(I_T/I_P)$, where I_T and I_P were the peak Na-currents, obtained with the test pulse and the prepulse, respectively. The ratio was plotted against the time interval. τ is the time constant of the exponential relationship obtained. Pipette and bath solutions were as in *A*. *D*, Voltage dependence of steady-state inactivation of the Na current (see text). The data points from two cells were fitted with Eq. 1 (drawn line), with $V_h = -50$ mV and $k = -6.5$ mV. Pipette and bath solutions were as in *A*.

voltage to deviate from the pipette clamp voltage. The corresponding data were not used for the analysis.

To study the voltage dependence of the steady-state inactivation, the largest peak current (I), obtained with pulsed depolarization from different holding voltages (V),

was normalized to I_{max}, obtained when the holding voltage was −80 mV. The plot of I/I_{max} as a function of V resulted in a sigmoid (Fig. 4 *D*), which was fitted with

$$I/I_{max} = 1/\{1 + \exp[(V - V_h)/k]\}, \quad (1)$$

where V_h is the half-inactivation voltage and k is the steepness coefficient. The values found were −50 mV and −6.5 mV, respectively. Recovery from inactivation, measured with a two-pulse protocol, could be fitted with a single exponential of time constant 2.82 ms at −80 mV. These results are in the range of those obtained for TTX-sensitive, voltage-gated Na currents in other preparations (see Hille, 1984).

Voltage-gated K Current

With inward currents suppressed by replacing the external Na with NMDG, outward currents were elicited with depolarizing pulses exceeding −30 mV. Fig. 5 *A* shows typical time courses with slow inactivation during prolonged depolarizations. The resulting current–voltage relationship for peak and steady-state currents is depicted in Fig. 5 *B*.

Amplitudes of tail currents were measured at −40 mV, after termination of graded depolarizing pulses (Fig. 5 *C*). Activation of the outward currents started at −30 mV and was complete at +5 mV. The activation curve was of sigmoid shape and could be fitted with Eq. 1. Half-activation occurred at −20 mV, and the steepness coefficient was 6 mV.

Fig. 5 *D* shows the blocking effects of classical K channel blockers. While 10 mM tetraethylammonium (TEA) reduced peak and steady-state currents uniformly, 5 mM 4-aminopyridine (4-AP) tended to block the peak current more efficiently. 10 mM Ba also blocked 50% of the K outward current (not shown). Thus, several K conductances with different pharmacological properties might be present in the TRCs.

Voltage-gated Inward Ca Currents

When CsCl or NMDG substituted for KCl in the pipette, the inactivation of inward current sometimes was incomplete, leaving a small stationary component. This component was enhanced when the Ca was increased to 10 mM (Fig. 6 *A*). The resulting steady-state current–voltage relationship (Fig. 6 *B*, solid symbols) revealed a sustained Ca current activating at −30 mV and having a reversal potential near 40 mV.

To study current through Ca channels with better resolution, we replaced the Na of the Tyrode solution with 100 mM Ba. Ba is known to pass Ca channels as well as or better than Ca (Bean, 1989). Furthermore, it blocks remaining outward K currents. Fig. 6 *C* shows the current time courses resulting from step depolarization from a holding voltage of −80 mV. Despite the presence of 2μM TTX and the absence of Na, a transient inward current was elicited at the threshold of −50 mV. The current inactivated completely within 75 ms at voltages of −50 to −20 mV. At higher depolarizations a more sustained inward current superimposed the time courses of the transient current. Thus the Ca current could be divided into a low threshold inactivating component, i.e., the T-type current (ICa_T), and a sustained component of higher threshold, the L-type current (ICa_L). It is difficult to distinguish the L-type from the N-type Ca channel (ICa_N) (Bean, 1989), and we are not

sure to what extent our ICa_L is contaminated by ICa_N. We are using the term ICa_L because of the slow inactivation with a time constant of 1.3 s occurring at 0 mV (Fig. 6 *E*), which is close to the value of 1.4 s found by Fox et al. (1987) at this voltage. In contrast, ICa_N inactivates with time constants <100 ms at 0 mV (Fox et al., 1987).

The currents remaining after inactivation of ICa_T were plotted against voltage (Fig.

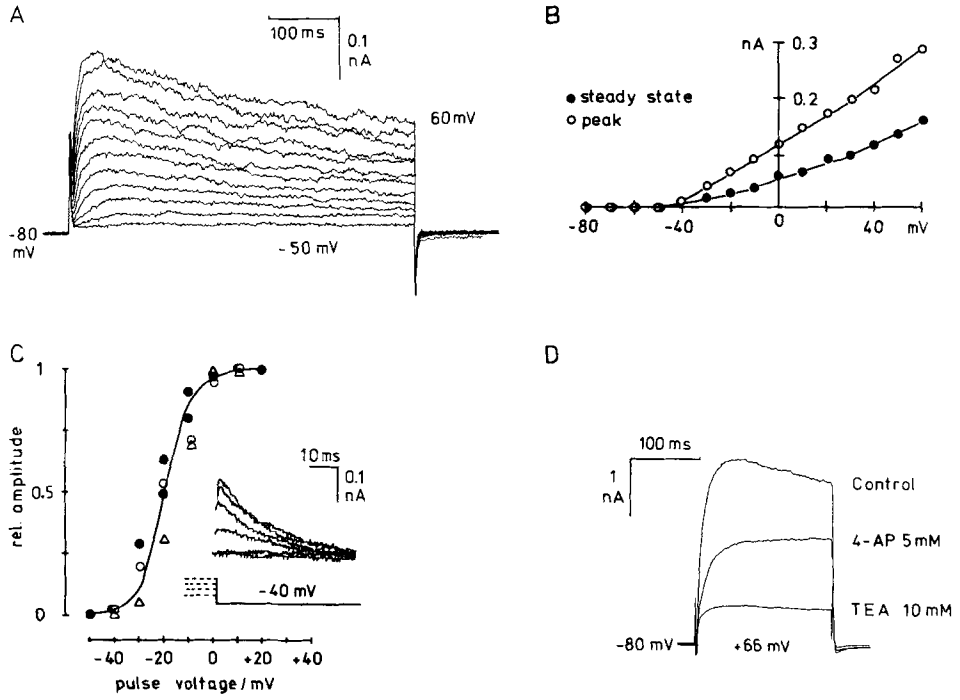

FIGURE 5. Outward K currents. *A*, Current time courses in response to depolarizing pulses (steps of 10 mV) from −80 mV to the voltages indicated. The pipette contained the standard KCl filling solution and the Na of the external Tyrode was replaced by NMDG. *B*, Peak and steady-state currents obtained under the conditions in *A*. The linear leak current (−33 pA at −80 mV) was subtracted. *C*, Voltage dependence of the K current activation. The amplitude of the tail current obtained at −40 mV at the end of 100-ms depolarizing pulses (see inset) was normalized with the maximal tail current and plotted against the command pulse voltage. The data points of three cells are fitted with Eq. 1 (*drawn line*), with $V_h = -20$ mV and $k = 6$ mV. Pipette and bath solutions were as in *A*. *D*, Blocking effects of 4-AP and TEA. Current time course obtained by depolarizing the TRC from −80 mV to +66 mV. The pipette contained the standard KCl solution and the external solution was Tyrode.

6 *D*) to obtain the current–voltage relationship for ICa_L. The values were then subtracted from the peak currents to obtain ICa_T. Both Ca currents peaked at 0 mV and had a rather low reversal potential (+50 mV), indicating that the channels are not purely selective to divalent cations, as was described for some other systems (see Reuter and Scholz, 1977; Hess et al., 1986; Pelzer et al., 1990).

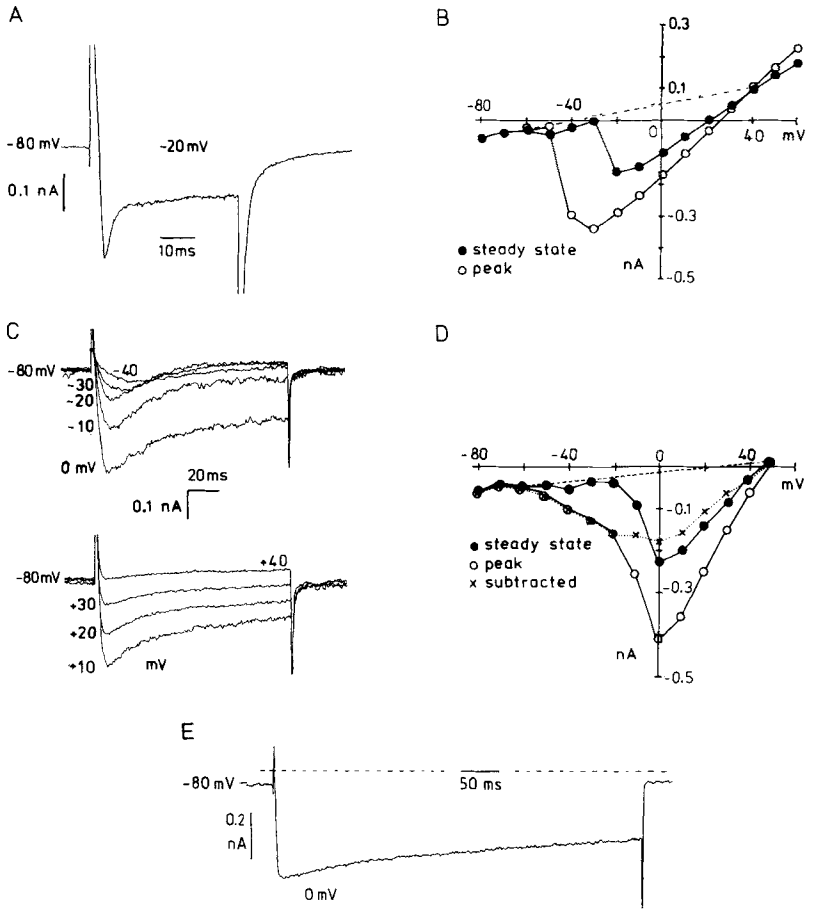

FIGURE 6. Ca currents. *A*, Current time course in response to a depolarization from −80 to −20 mV (capacitive currents were not compensated). The K of the standard pipette solution was replaced by NMDG and 10 mM $CaCl_2$ was added to the external Tyrode solution. *B*, Peak and steady-state currents obtained under the conditions in *A*. The leakage current (evaluated by the linear slope in the negative voltage range) is represented by the dashed line. The curves cross the leakage current at a reversal potential of 40 mV. *C*, Current time courses in response to depolarizing pulses from −80 mV to the voltages indicated when the external solution contained 100 mM $BaCl_2$, 10 mM HEPES (pH 7.4), 2 μM TTX, and the K of the pipette solution was replaced by NMDG. *D*, Current–voltage relationship obtained with the cell of *C* under the same conditions. The steady-state component, measured at the end of the pulse, does not include the fast inactivating ICa_T and represents ICa_L. *Dashed line,* linear leak current; *dotted line,* difference between peak and steady-state current representing ICa_T. *E*, Time course of ICa_L in response to a pulse from −80 to 0 mV. The K of the pipette solution was replaced by NMDG and the external solution was the high Ba solution of *C* to which 0.2 mM $NiCl_2$ was added to block ICa_T (see Fig. 7). The slow inactivation had a time constant of 1.3 s.

0.2 mM Ni fully blocked $I\text{Ca}_T$ but did not affect $I\text{Ca}_L$. In Fig. 7 *A* the Ni-sensitive current ($I\text{Ca}_T$) was determined by subtracting the curve obtained under full block of Ni from the control curve. Both currents were blocked by 0.5 mM Cd (Fig. 7, *B* and *C*), but whereas $I\text{Ca}_L$ almost completely disappeared at this blocker concentration, $I\text{Ca}_T$ was reduced by only 60%. Similarly, the Ca channel blocker D600 reduced $I\text{Ca}_L$ by 76% at 50 μM and blocked only 50% of $I\text{Ca}_T$ (Fig. 7, *B* and *C*).

From a total of 42 cells tested for Ca currents, 35 had inward Na currents (measured in Tyrode) and 27 had inward currents in 100 mM Ba. While $I\text{Ca}_T$ and $I\text{Ca}_L$ were present simultaneously in 11 cells, 16 TRCs had only $I\text{Ca}_T$. The peak

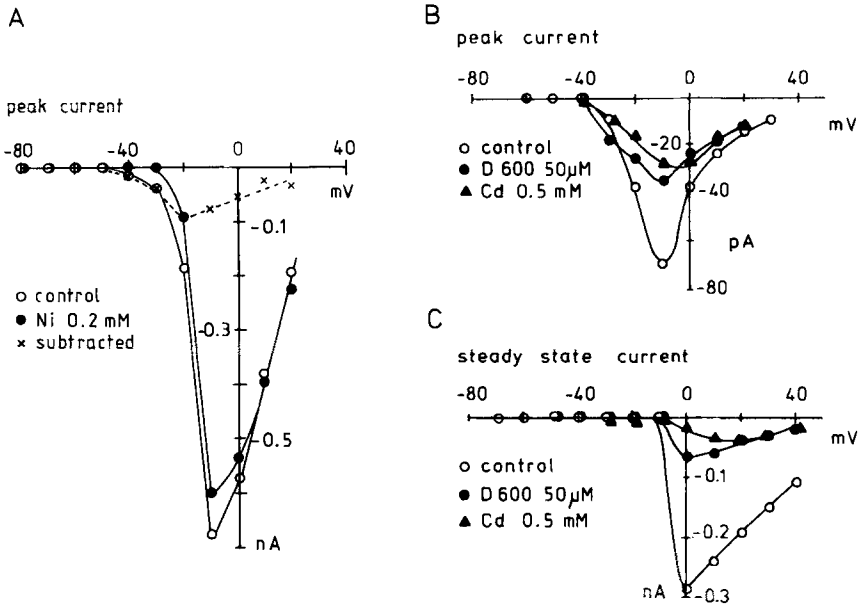

FIGURE 7. Differential blockage of L- and T-type Ca currents. *A*, Current–voltage relationship of the peak current in the presence and absence of Ni (0.2 mM). *Open circles*, $I\text{Ca}_L$ + $I\text{Ca}_T$; *solid circles*, $I\text{Ca}_L$ remained when $I\text{Ca}_T$ was blocked with 0.2 mM Ni; *dashed line*, $I\text{Ca}_T$ obtained by subtraction. The leak current was also subtracted. The pipette contained NMDG instead of K and the bath was the high Ba solution of Fig. 6. *B* and *C*, Blocking effects of D600 and Cd on the peak current, $I\text{Ca}_T$ (*B*) and the steady-state current, $I\text{Ca}_L$ (*C*). Solutions were as in *A*.

current was 53 ± 40 pA (27) for $I\text{Ca}_T$ and 440 ± 297 pA (11) for $I\text{Ca}_L$. Among the cells having Ca currents, $I\text{Ca}_L$ was absent in 60% of the cases, probably due to a fast rundown (Byerly and Hagiwara, 1982; Fenwick et al., 1982*a*; Belles et al., 1988). However, this finding allowed us to study $I\text{Ca}_T$ separately, as will be seen in the next section.

T-Type Ca Current

The time course of the T-type calcium current resulting from pulsed depolarizations is shown in Fig. 8 *A*. Compared with the Na current, the activation was slower (time

to peak 20 ms at −30 mV). The threshold for activation was in the range −50 to −40 mV and the peak currents plotted versus pulse voltage gave a bell-shaped curve with a maximum ranging between −30 and 0 mV (Fig. 8 *B*). The reversal potential was clearly less positive than would be expected for a pure Ba-Ca selectivity (300 mV).

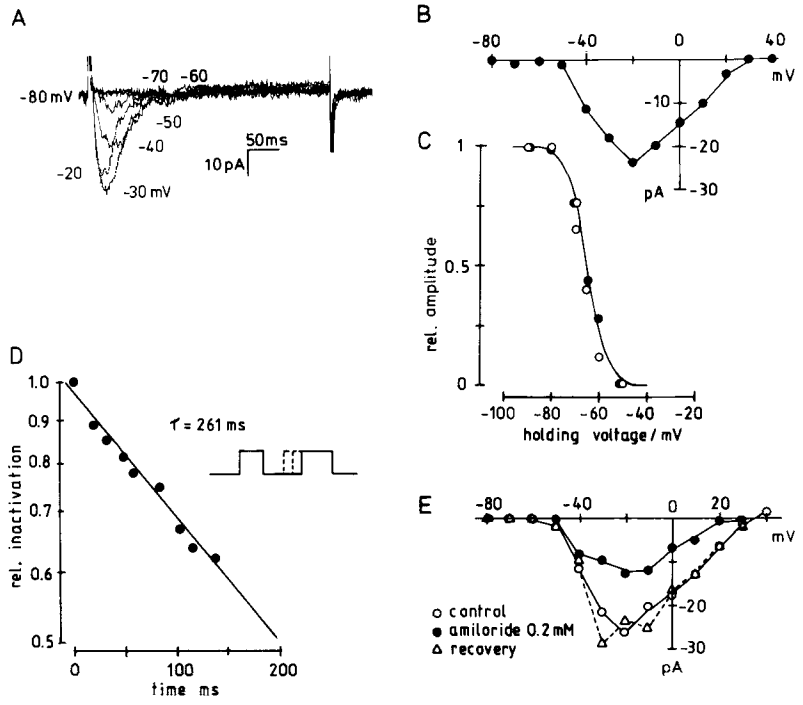

FIGURE 8. The transient inward Ca current. *A*, Current time course (ICa_T) in response to step depolarizations (as indicated) from a −80 mV holding potential in a TRC having no ICa_L. The pipette contained NMDG instead of K and the outer solution was (in mM): 100 $BaCl_2$, 10 HEPES (pH 7.4). *B*, Current–voltage relationship obtained under the conditions in *A*. The linear leak was subtracted. *C*, Voltage dependence of the steady-state inactivation of ICa_T. The protocol was the same as for the transient Na current. The data points obtained from two cells were fitted with Eq. 1 (drawn line), yielding $V_h = -65$ mV and $k = -4$ mV. *D*, Recovery from inactivation of ICa_T at −80 mV. The protocol was the same as for the Na transient current in Fig. 4 *C*. Prepulse and test pulse to 0 mV from a −80 mV holding voltage. τ is the time constant of the exponential relationship obtained. Pipette and bath solutions were as in *A*. *E*, Blocking effect of amiloride (0.2 mM) on ICa_T. The current–voltage relationships were obtained as described for *B*.

The current inactivated at −30 mV with a time constant of 36 ms. The slow recovery from inactivation, studied with a double-pulse protocol, could be approximated with a single exponential of 261 ms time constant (Fig. 8 *D*). The voltage dependence of the inactivation was studied with the protocol previously used for the

Na current and the resulting curve was fitted with Eq. 1. The half-inactivation was −65 mV and the steepness coefficient was −4 mV (Fig. 8 *C*).

It has recently been shown that amiloride, a blocker of the common epithelial Na channel, blocks the T-type Ca channel of neuroblastoma cells. The reported inhibition constant was 30 μM (Tang et al., 1988). In our experiments amiloride also blocked $I\text{Ca}_\text{T}$. However, the apparent inhibition constant was relatively high, in the order of 200 μM (Fig. 8 *E*).

Influence of the External Divalent Cation Concentration

Replacing Ba with Ca reduced $I\text{Ca}_\text{L}$ by 50% but did not reduce $I\text{Ca}_\text{T}$. L-type Ca channels are commonly observed to have a higher premeability for Ba than for Ca. Thus, as far as the kinetic and pharmacological properties are concerned, $I\text{Ca}_\text{T}$ and $I\text{Ca}_\text{L}$ of TRCs resemble the two types of Ca current classically described in other excitable cells (for review see Bean, 1989). Their activation thresholds, however, are 20 mV more positive than the values of −70 and −40 mV usually reported for $I\text{Ca}_\text{T}$ and $I\text{Ca}_\text{L}$, respectively.

This difference may be due to neutralization of surface charges by the high Ba or Ca concentration needed to reveal the currents (Hille, 1984; McDonald et al., 1986; Akaike et al., 1989). When the external Ca was reduced, a lowering of the threshold, concomitant with a decrease of the current amplitude, was observed (Fig. 9). As expected, the shift was more pronounced for changes in the low concentration range (Hille, 1984). At 3 mM external Ca the threshold was between −40 and −50 mV for $I\text{Ca}_\text{L}$, a value also found in other cells (see Bean, 1989). A similar shift was also observed for $I\text{Ca}_\text{T}$, but due to its small amplitude the current could not be studied below 50 mM external Ca.

Action Potentials in Response to Sweet Stimulation

As shown above, the taste cells from the rat fungiform papilla generate action potentials. Are these action potentials part of the normal response to a taste stimulus? To investigate this point we stimulated the cells with saccharin, which is a sweet agent also in the rat (Sato, 1971), and effective at moderate concentrations. Fig. 10 *A* shows the effect of superfusing a taste cell with 20 mM Na-saccharin in the cell-attached configuration. Saccharin induced an increase in outward current of ~2 pA, as recorded through the unbroken patch. It appears possible that a depolarization effected by saccharin was driving additional current through the leak conductance of the patch. (The conductance of on-cell patches can be much larger than predicted from whole-cell conductance and patch area [Fenwick et al., 1982*a*; Fischmeister et al., 1986]). However, a change in patch current induced by saccharin via second messenger is not excluded.

Action potentials were fired at a mean frequency of 0.6 s^{-1} during the period of depolarization. They became noticeable on the record as short biphasic current transients. The shape (see inset) indicated type II action potentials, i.e., those with a slow repolarization phase. The stimulatory effect of saccharin was reversible (repeated three times with the TRC of Fig. 10 *A*). Depolarization caused by saccharin was indicated in 24 out of 64 cells (38%) in the cell-attached configuration. Of the 24 cells, 7 fired action potentials.

A depolarization accompanied by action potentials was also observed in whole-cell recordings, as shown in Fig. 10 *B*. Of 38 cells tested, 14 (32%) responded to saccharin with a depolarization (mean amplitude 8.9 ± 5.1 mV), but only 2 fired action potentials. Thus it appears that the whole-cell mode is less suitable for observing this phenomenon than the on-cell mode.

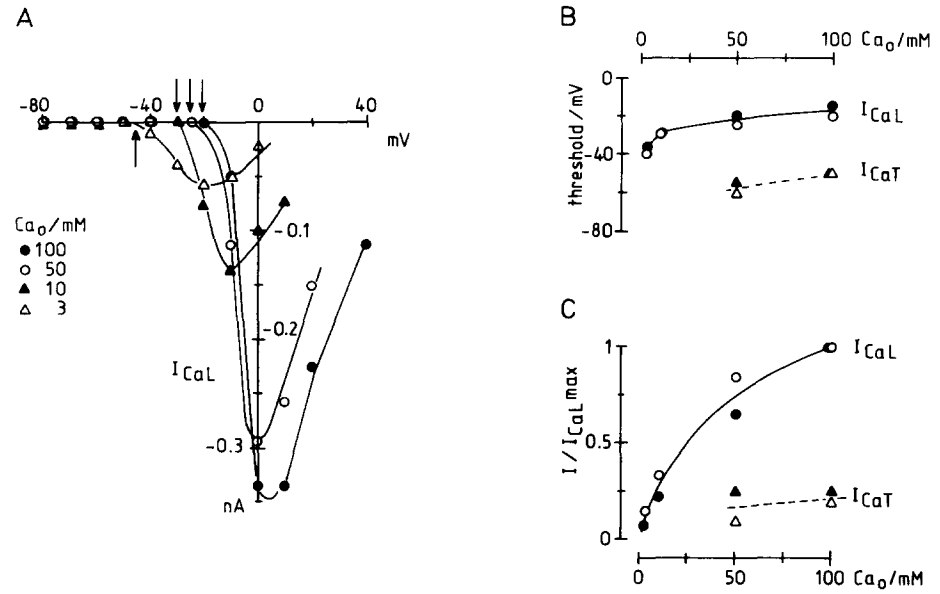

FIGURE 9. Effect of the concentration of external divalent cations on ICa_T and ICa_L. *A*, Near-stationary current–voltage relationships for ICa_L (obtained as in the preceding figures) at concentrations of Ca indicated. The arrows point to the threshold of activation of ICa_L. For Ca concentrations <100 mM the tonicity was adjusted with NMDG. The pipette contained NMDG instead of K. *B*, Threshold for activation of ICa_L and ICa_T as a function of external Ca for two cells under the conditions in *A*. *C*, Relative amplitude of ICa_L and ICa_T (maximal peak currents) as a function of external Ca (3–100 mM) of the two cells in *C*. The currents of each cell were normalized to the amplitude of ICa_L (ICa_{Lmax}) measured in 100 mM Ca.

Response of K Conductance to Sweet Stimulation

To identify the conductance responsible for the sweet-induced depolarization, quasi-simultaneous currents were recorded at the reversal potentials of the three principal ions: Na (+66 mV), Cl (0 mV), and K (−80 mV). In whole-cell voltage clamp the potential was stepped every 3 s from a holding voltage of −80 mV (close to the reversal potential for K). A computer generated the command pulses of 30–40 ms duration (Fig. 11 *A*) and sampled the currents continuously at 1 kHz. Values toward the end of each voltage were stored in separate arrays and displayed as separate current traces.

The method of interleaved recording was first tested with TEA (Fig. 11 *B*). The K channel blocker caused a reversible decrease of the currents at the reversal potentials of Na and Cl but did not affect the current measured at the K reversal potential. A

similar reversible reduction of outward currents at the Cl and Na reversal potentials was found during superfusion with saccharin (Fig. 11, *C* and *D*). There was no change at the K reversal potential, indicating that the Na content of the 20 mM Na-saccharin addition was not relevant for the response. Rather, the results indicate that a decrease in the K conductance was responsible for the decrease in the outward current. A reduction of K current was observed in 34% of the 55 cells tested and averaged 21 ± 7%.

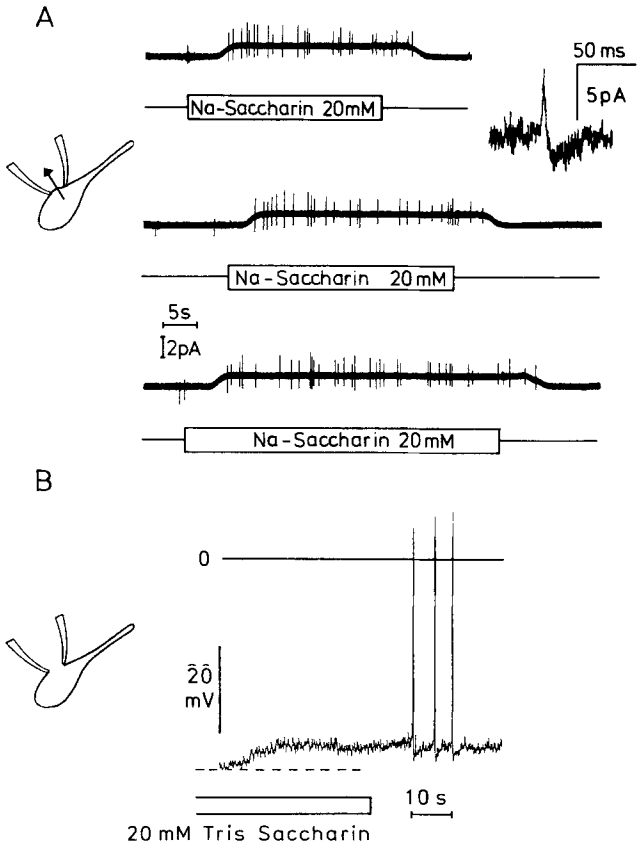

FIGURE 10. Response to saccharin. *A*, Cell-attached recording of the patch current during slow superfusion with saccharin (20 mM). Current flowing from the cell to the pipette is plotted upward. Action potentials are indicated by fast current transients (see inset). The pipette contained the standard KCl filling solution and the bath was Tyrode. *B*, Whole-cell current clamp recording during slow superfusion of saccharin (20 mM). Washout of saccharin took 65 s. Solutions were the same as in *A*.

A decrease in K conductance in response to a cAMP-mediated phosphorylation was demonstrated in frog TRCs (Avenet et al., 1988). In rat TRCs bath application of 5 mM cAMP produced a 14 ± 7% decrease of the K conductance in 10 of 25 saccharin-responsive cells (Fig. 11, *C* and *D*). The yield was not improved when 8-Br cAMP, di-but-cAMP, or cpt-cAMP were used, when 0.1 mM IBMX was added, or

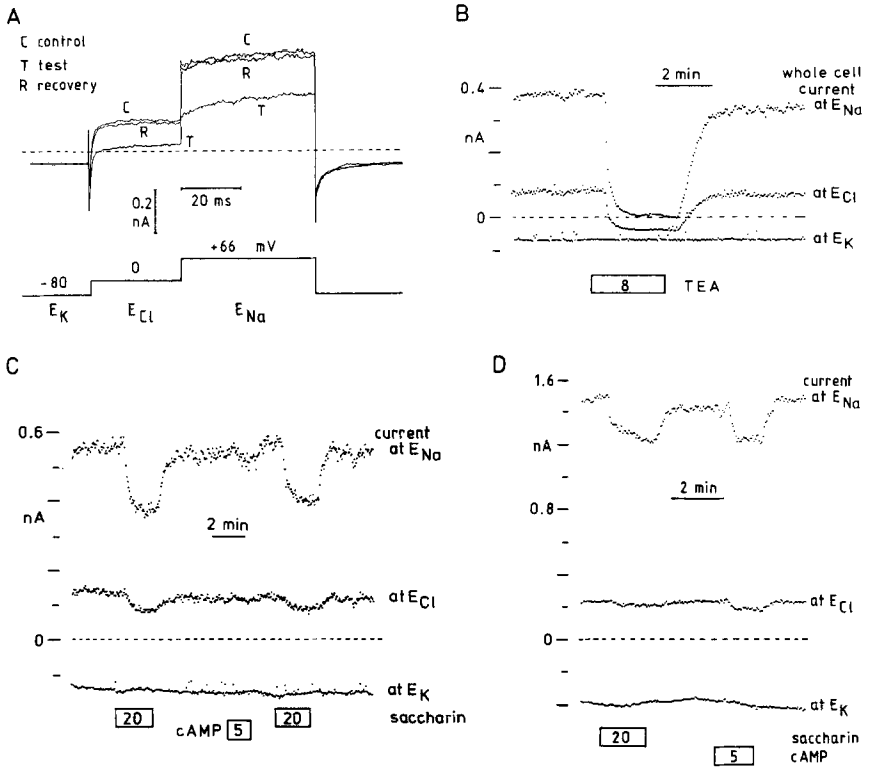

FIGURE 11. Interleaved (quasi-simultaneous) recording of current at three voltages. *A*, Pulse protocol (lower trace) and corresponding current time course (upper trace) used to analyze the current changes in response to superfusion with various agents added to the Tyrode solution (in this example it was 20 mM saccharin). The voltage values −80, 0, and +66 mV correspond to the equilibrium potentials of K, Cl, and Na. The pulse protocol was repeated every 3 s and the mean current over 10 ms at the end of each voltage pulse was used for the time course display of *B*, *C*, and *D* (see text). The pipette always contained the standard KCl filling solution. *B*, Test of method: time course of the whole-cell current at the equilibrium potentials for Na (E_{Na}), Cl (E_{Cl}), and K (E_K) in response to a slow superfusion of TEA (8 mM). Note that the currents are affected at E_{Na} and E_{Cl} but not at E_K, suggesting that the current blocked by TEA was K current. *C*, Another cell: time course of the whole-cell currents during slow superfusion with saccharin and cAMP. *D*, Another cell under the same conditions as in *C*. Note that the effects of saccharin and cAMP are similar in *D* but not in *C*.

when the patch was permeabilized with nystatin. No attempt was made here to characterize further the TEA-blockable K channels that close in response to saccharin.

DISCUSSION

Characteristics of the TRCs

The shape of rat TRCs, as observed after micro-dissection, is comparable to amphibian TRCs (Kinnamon et al., 1988; Richter et al., 1988) and shows a typical

elongated apical pole. Rat TRCs are, however, thinner (30 μm in length, 4 μm wide at the soma, and 1 μm at the apical pole), which explains their smaller membrane capacitance of 3–5 pF. A membrane capacitance of 10 pF was measured for frog TRCs (Avenet and Lindemann, 1987*b*) and 50 pF for *Necturus* (Kinnamon and Roper, 1988).

The method used to prepare rat TRCs suitable for patch clamping produced cells that seemed viable inasmuch as they still generated action potentials. Indeed, the fact that action potentials were recorded in the on-cell mode, i.e., without first loading the cell with K from the pipette solution, demonstrates the low Na, high K content of TRCs and their high resting potential. This was achieved by lowering the metabolic rate (4°C at reduced K gradient) while the cells were prepared. Minimal enzyme exposure and a fast protocol were also essential.

In amphibian TRCs the presence of voltage-gated conductances and the ability to generate action potentials was previously demonstrated with micro-electrode impalements (Kashiwayanagi et al., 1983; Roper, 1983; Avenet and Lindemann, 1987*a*), and more recently with the patch clamp technique (Avenet and Lindemann, 1987*b;* Kinnamon and Roper, 1988; Miyamoto et al., 1988; Teeter et al., 1989). Less patch clamp data are available for mammals. In the rat, only 10% of TRCs isolated from the circumvallate papilla were reported to have a transient Na inward current (Akabas et al., 1988, 1990), whereas in the mouse this current was present in half of the cells (Spielman et al., 1989).

From the four types of cells described in mammalian taste buds (basal cell, type I or dark cell, type II or light cell, and perigemmal cell), type I (representing 50–70% of the cells) are believed to have receptor functions (Farbman, 1965; Murray, 1971). In our study the transient Na current was present in 72% of the cells patched. Thus, the number of electrically excitable cells roughly matches the number of putative receptor cells. Cells from the periphery as well as from more central positions in the taste buds were patched. However, no correlation between the topology and the presence of one or several voltage-gated conductances was observed.

Two Types of Ca Currents

While a quasi-L-type Ca current was found in amphibian TRCs (Kinnamon and Roper, 1988), Ca currents were not previously demonstrated in the mammalian taste buds (Spielman et al., 1989; Akabas et al., 1990). Here we report that TRCs from the rat fungiform papilla have a low and high threshold calcium current, as in a variety of other excitable cells (for review see Bean, 1989). The current density of $I\mathrm{Ca}_\mathrm{L}$ of 15 pA/pF in 10 mM Ca was smaller than the current density measured in *Necturus* taste cells (32 pA/pF in 10 mM Ca; Kinnamon and Roper, 1988) or in adrenal chromaffin cells (33 pA/pF in 5 mM Ca; Fenwick et al., 1982*b*) but similar to the density found in pancreatic β cells (12 pA/pF in 10 mM Ca; Rorsman and Trube, 1986). $I\mathrm{Ca}_\mathrm{T}$ represented only 25% of the current density of $I\mathrm{Ca}_\mathrm{L}$ (measured in Ca), a value typically observed for other cells (Bossu et al., 1985; Fedulova et al., 1985; Carbone and Lux, 1987; Fox et al., 1987).

It has been suggested that $I\mathrm{Ca}_\mathrm{T}$ plays a role in the membrane potential oscillations of certain central neurons (Coulter et al., 1989; Crunelli et al., 1989), in pituitary cells (Matteson and Armstrong, 1986), or in α_2 pancreatic cells (Rorsman, 1988). Its

low threshold (close to the resting potential) and the presence of Ca-dependent K channels make $I\mathrm{Ca}_T$ suitable for generation of bursting or pacemaker activities. In TRCs we did not observe potential oscillations. It cannot be excluded that such a behavior was suppressed by an alteration during cell dissociation.

A role of amplifier for low efficiency depolarization in sensory neurons and α_2 pancreatic cells has also been suggested (Bossu et al., 1985; Rorsman, 1988) for $I\mathrm{Ca}_T$. In TRCs, $I\mathrm{Ca}_T$ would be activated by receptor potentials of small amplitude and then would cause further depolarization up to the excitation threshold. Alternatively, $I\mathrm{Ca}_T$ would allow Ca entry in cells unable to produce a fully developed action potential. Finally, $I\mathrm{Ca}_T$ is often found in embryonic and immature cells and a role in development was proposed. In the taste bud there is a continuous renewal of the cells (Delay et al., 1986). Thus the presence of $I\mathrm{Ca}_T$ may reflect an early stage of maturation.

In contrast to the "electrical" functions of $I\mathrm{Ca}_T$, and $I\mathrm{Ca}_L$ and more recently $I\mathrm{Ca}_N$ were implicated in secretory processes (Rane et al., 1987; Hirning et al., 1988). When these Ca channels are opened, inflow of Ca leads to fusion of secretory vesicles with the plasma membrane. In presynaptic terminals, $I\mathrm{Ca}_N$ is more likely than $I\mathrm{Ca}_L$ to trigger transmitter release (Miller, 1987; but see Maguire et al., 1989). Similarly, in the taste cells of fungiform papillae $I\mathrm{Ca}_L$ and/or $I\mathrm{Ca}_N$ may trigger transmitter release at the synapse with the sensory axon. This is in contrast to bitter-sensitive cells of the circumvallate papilla, where the rise of cytosolic Ca is due to release from intracellular stores (Akabas et al., 1988).

L-type Ca currents are often subject to extensive regulation. $I\mathrm{Ca}_L$ of TRCs might be directly under the control of a second messenger as, for instance, the beta-adrenoreceptor pathway in cardiocytes (Kameyama et al., 1985; Pelzer et al., 1990). This possibility remained unexplored in this study.

Why Do Taste Cells Fire Action Potentials?

We show that taste cells are able to fire action potentials in response to sweet stimulation. Similar responses of amphibian taste cells to sour and salty have been recorded previously (Avenet and Lindemann, 1987*a;* Kinnamon and Roper, 1987). Thus the use of voltage-gated conductances as part of the signalling chain is now demonstrated for TRCs of several vertebrates. This contradicts previous microelectrode studies, where taste cells, including those of the rat, were found to be nonexcitable (see Sato, 1980). The discrepancy may be explained by damage during microelectrode impalement.

The presence of one Na and two Ca voltage-gated currents confer to the taste cells electrical properties similar to those of other chemosensitive cells as, for example, the glucagon-secreting α_2 pancreatic cells (Rorsman, 1988) or the O_2-sensitive cells of the carotid body (Urena et al., 1989). Like these cells, TRCs are "short" and their action potentials are obviously not needed for impulse propagation. Rather, they may serve to depolarize the membrane, from receptor potentials of small amplitude, sufficiently to fully activate $I\mathrm{Ca}_L$. Indeed, the low density of Ca currents found in the rat TRCs may not be sufficient for a pure regenerative Ca action potential leading to full activation of the Ca currents. Therefore, a Na action potential is required to

bridge the gap between the receptor potential and the threshold of ICa_L (Avenet and Lindemann, 1989), to assure optimal Ca influx and transmitter release.

Response to Sweet

A subpopulation (34%) of rat TRCs responded to Na saccharin with a depolarization linked to a decrease in outward K currents. A decrease in K currents in response to sucrose was also reported for the "type H" TRCs of the mouse, while "type D" appeared to respond with an increase in Na conductance (Tonosaki and Funakoshi, 1984). Thus, more than one transduction pathway for "sweet" may exist in TRCs of rodents. A pathway of sweet-transduction involving the opening of a nonspecific apical conductance was indicated for the dog (Mierson et al., 1988; Simon et al., 1989).

In mouse TRCs, injected cyclic nucleotides, like exposure to sucrose, induced depolarization and a decrease in membrane conductance (Tonosaki and Funakoshi, 1988). For the rat, an adenylate cyclase stimulated by sweet agents was reported (Striem et al., 1989), and intact taste cells were recently shown to generate cAMP in response to exposure with sucrose (Striem et al., 1990). In the frog, cAMP caused an inhibition of outward current and a depolarization in ~50% of the TRCs investigated (Avenet and Lindemann, 1987*b*). For frog taste cells, a closure of 44 pS K channels by cAMP-activated phosphorylation was demonstrated and was suggested to participate in the transduction mechanism for the sweet taste (Avenet et al., 1988). We now found in some rat TRCs responding to saccharin that added cAMP, like saccharin, reduced the outward K current (Fig. 11 *D*). However, only 40% of the cells responding to saccharin also responded to cAMP. Further work is needed to elucidate this point.

Taste cells were often described as "multimodal," broadly tuned receptors (for a review, see Avenet and Lindemann, 1989). One would then expect that most TRCs respond to some extent to sweet stimuli. The fact that the response was observed in only 34% of the TRCs might be due to a subtle alteration of the cells in response to dissociation. The elucidation of this point will need further work, probably with noninvasive techniques like recording from intact tissue (Béhé et al., 1989*b*).

Our thanks are due to Frau Stephanie Theiss and to Frau Katrin Sandmeyer for technical assistance and to Herrn Gert Ganster for construction and servicing of electronics.

Support was obtained from the Deutsche Forschungsgemeinschaft through SFB 246, project C1 and from the Campbell Institute for Research and Technology.

Original version received 16 March 1990 and accepted version received 4 June 1990.

REFERENCES

Akabas, M. H., J. Dodd, and Q. Al-Awqati. 1988. A bitter substance induces rise in intracellular calcium in a subpopulation of rat taste cells. *Science.* 242:1047–1050.

Akabas, M. H., J. Dodd, and Q. Al-Awqati. 1990. Identification of electrophysiologically distinct subpopulations of rat taste cells. *Journal of Membrane Biology.* 114:71–78.

Akaike, N., P. G. Kostyuk, and Y. V. Osipchuk. 1989. Dihydropyridine-sensitive low-threshold calcium channels in isolated rat hypothalamic neurones. *Journal of Physiology.* 412:181–195.

Avenet, P., F. Hofman, and B. Lindemann. 1988. Transduction in taste receptor cells requires cAMP-dependent protein kinase. *Nature.* 331:351–354.

Avenet, P. and B. Lindemann. 1987*a*. Action potentials in epithelial taste receptor cells induced by mucosal calcium. *Journal of Membrane Biology.* 95:265–269.

Avenet, P., and B. Lindemann. 1987*b*. Patch-clamp study of isolated taste receptor cells of the frog. *Journal of Membrane Biology.* 97:223–240.

Avenet, P., and B. Lindemann. 1989. Perspectives of taste reception. *Journal of Membrane Biology.* 112:1–8.

Bean, B. P. 1989. Classes of calcium channels in vertebrate cells. *Annual Review of Physiology.* 51:367–384.

Béhé, P., J. A. DeSimone, P. Avenet, and B. Lindemann. 1989*a*. Patch-clamp recordings from isolated rat taste buds: responses to saccharin and amiloride. Xth International Symposium of Olfaction and Taste (ISOT), Oslo. 270. (Abstr.)

Béhé, P., J. A. DeSimone, P. Avenet, and B. Lindemann. 1989*b*. Patch-clamp recordings from taste buds of maintained epithelial polarity: a novel approach. Xth International Symposium of Olfaction and Taste (ISOT), Oslo. 271. (Abstr.)

Belles, B., C. O. Malécot, J. Hescheler, and W. Trautwein. 1988. "Run-down" of the Ca current during long whole-cell recordings in guinea pig heart cells: role of phosphorylation and intracellular calcium. *Pflügers Archiv.* 411:353–360.

Bossu, J. L., A. Feltz, and J. M. Thomann. 1985. Depolarization elicits two distinct calcium currents in vertebrate sensory neurones. *Pflügers Archiv.* 403:360–368.

Byerly, L., and S. Hagiwara. 1982. Calcium currents in internally perfused nerve cell bodies of *Limnea stagnalis*. *Journal of Physiology.* 322:503–528.

Carbone, E., and H. D. Lux. 1987. Kinetics and selectivity of a low-voltage-activated calcium current in chick and rat sensory neurones. *Journal of Physiology.* 386:547–570.

Coulter, D. A., J. R. Huguenard, and D. A. Prince. 1989. Calcium currents in rat thalamocortical relay neurones: kinetic properties of the transient, low threshold current. *Journal of Physiology.* 414:587–604.

Crunelli, V., S. Lightowler, and C. E. Pollard. 1989. A T-type Ca current underlies low-threshold Ca potentials in cells of the cat and rat lateral geniculate nucleus. *Journal of Physiology.* 413:543–561.

Delay, R. J., J. C. Kinnamon, and S. D. Roper. 1986. Ultrastructure of mouse vallate taste buds. II. Cell types and cell lineage. *Journal of Comparative Neurology.* 277:242–252.

Farbman, A. I. 1965. Fine structure of the taste bud. *Journal of Ultrastructure Research.* 12:328–350.

Fedulova, S. A., P. G. Kostyuk, and N. S. Veselovsky. 1985. Two types of calcium channels in the somatic membrane of new-born rat dorsal root ganglion neurones. *Journal of Physiology.* 359:431–446.

Fenwick, E. M., A. Marty, and E. Neher. 1982*a*. A patch-clamp study of bovine chromaffin cells and of their sensitivity to acetylcholine. *Journal of Physiology.* 331:577–597.

Fenwick, E. M., A. Marty, and E. Neher. 1982*b*. Sodium and calcium channels in bovine chromaffin cells. *Journal of Physiology.* 331:599–635.

Fischmeister, R., R. K. Ayer, Jr., and R. L. DeHaan. 1986. Some limitations of the cell-attached patch clamp technique: a two-electrode analysis. *Pflügers Archiv.* 406:73–82.

Fox, A. P., M. C. Nowycky, and R. W. Tsien. 1987. Kinetic and pharmacological properties distinguishing three types of calcium currents in chick sensory neurones. *Journal of Physiology.* 394:149–172.

Hamill, O. P., A. Marty, E. Neher, B. Sakmann, and F. J. Sigworth. 1981. Improved patch-clamp techniques for high-resolution current recording from cells and cell-free membrane patches. *Pflügers Archiv.* 391:85–100.

Hammes, G. G., and S. E. Schullery. 1970. Structure of macromolecular aggregates. II. Construction of model membranes from phospholipids and polypeptides. *Biochemistry.* 9:2555–2563.

Hess, P., J. B. Lansman, and R. W. Tsien. 1986. Calcium channel selectivity for divalent and monovalent cations. Voltage and concentration dependence of single channel current in ventricular heart cells. *Journal of General Physiology.* 88:293–319.

Hille, B. 1984. Ionic Channels of Excitable Membranes. Sinauer Associates, Inc., Sunderland, MA. 303–353.

Hirning, L. D., A. P. Fox, E. W. McCleskey, B. M. Olivera, S. A. Thayer, R. J. Miller, and R W. Tsien. 1988. Dominant role of N-type Ca channel in evoked release of norepinephrine from sympathetic neurons. *Science.* 239:57–61.

Horn, R., and A. Marty. 1988. Muscarinic activation of ionic currents measured by a new whole-cell recording method. *Journal of General Physiology.* 92:145–159.

Ivens, I., and J. W. Deitmer. 1986. Inhibition of a voltage-dependent Ca current by concanavalin A. *Pflügers Archiv.* 406:212–217.

Kameyama, M., F. Hofmann, and W. Trautwein. 1985. On the mechanism of β-adrenergic regulation of the Ca channel in the guinea-pig heart. *Pflügers Archiv.* 405:285–293.

Kashiwayanagi, M., M. Miyake, and K. Kurihara. 1983. Voltage-dependent Ca channel and Na channel in frog taste cells. *American Journal of Physiology.* 244:C82–C88.

Kinnamon, S. C., T. A. Cummings, and S. D. Roper. 1988. Isolation of single taste cells from lingual epithelium. *Chemical Senses.* 13:355–366.

Kinnamon, S. C., and S. D. Roper. 1987. Passive and active membrane properties of mudpuppy taste receptor cells. *Journal of Physiology.* 383:601–614.

Kinnamon, S. C., and S. D. Roper. 1988. Membrane properties of isolated mudpuppy taste cells. *Journal of General Physiology.* 91:351–371.

Maguire, G., B. Maple, P. Lukasiewicz, and F. Werblin. 1989. Gama-aminobutyrate type B receptor modulation of L-type calcium channel current at bipolar cell terminals in the retina of the tiger salamander. *Proceedings of the National Academy of Sciences USA.* 86:10144–10147.

Matteson, D. R., and C. M. Armstrong. 1986. Properties of two types of calcium channels in clonal pituitary cells. *Journal of General Physiology.* 87:161–182.

McDonald, T. F., A. Cavalié, W. Trautwein, and D. Pelzer. 1986. Voltage-dependent properties of macroscopic and elementary calcium channel currents in guinea pig ventricular myocytes. *Pflügers Archiv.* 406:437–448.

Mierson, S., S. K. DeSimone, G. L. Heck, and J. A. DeSimone. 1988. Sugar-activated ion transport in canine lingual epithelium. Implications for sugar taste transduction. *Journal of General Physiology.* 92:87–111.

Miller, R. J. 1987. Multiple calcium channels and neuronal function. *Science.* 235:46–52.

Miyamoto, T., Y. Okada, and T. Sato. 1988. Membrane properties of isolated frog taste cells: three types of responsivity to electrical stimulation. *Brain Research.* 449:369–372.

Murray, R. G. 1971. Ultrastructure of taste receptors. *In* Handbook of Sensory Physiology. Vol. IV. L. M. Beidler, editor. Springer-Verlag New York Inc., New York. 31–50.

Pelzer, D., S. Pelzer, and T. F. McDonald. 1990. Properties and regulation of calcium channels in muscle cells. *Review of Physiological and Biochemical Pharmacology.* 114:107–207.

Rane, S. G., G. G. Holtz IV, and K. Dunlap. 1987. Dihydropyridine inhibition of neuronal calcium current and substance P release. *Pflügers Archiv.* 409:361–366.

Reuter, H., and H. Scholz. 1977. A study of the ion selectivity and the kinetic properties of the Ca dependent slow inward current in mammalian cardiac muscle. *Journal of Physiology.* 264:17–47.

Richter, H.-P., P. Avenet, P. Mestres, and B. Lindemann. 1988. Gustatory receptors and neighbouring cells in the surface layer of an amphibian taste disc: in situ relationships and response to cell isolation. *Cell and Tissue Research.* 254:83–96.

Roper, S. D. 1983. Regenerative impulses in taste cells. *Science.* 220:1311–1312.

Rorsman, P. 1988. Two types of Ca currents with different sensitivities to organic Ca channel antagonists in guinea pig pancreatic α_2 cells. *Journal of General Physiology.* 91:243–254.

Rorsman, P., and G. Trube. 1986. Calcium and delayed potassium currents in mouse pancreatic β-cells under voltage clamp conditions. *Journal of Physiology.* 374:531–550.

Sato, M. 1971. Neural coding in taste as seen from recordings from peripheral receptors and nerves. *In* Handbook of Sensory Physiology. Vol. IV. L. M. Beidler, editor. Springer-Verlag New York Inc., New York. 116–147.

Sato, T. 1980. Recent advances in the physiology of taste cells. *Progress in Neurobiology.* 14:25–67.

Simon, S. A., P. Labarca, and R. Robb. 1989. Activation by cations of a cation-selective pathway on canine lingual epithelium. *American Journal of Physiology.* 256:R394–R402.

Spielman, A. I., I. Mody, J. G. Brand, G. Whitney, J. F. MacDonald, and M. W. Salter. 1989. A method for isolating and patch clamping single mammalian taste receptor cells. *Brain Research.* 503:326–329.

Striem, B. J., M. Naim, and B. Lindemann. 1990. Intracellular generation of cyclic AMP in the circumvallate taste buds of the rat in response to extracellular stimulation by sucrose. IXth Congress of the ECRO, Amsterdam. 97. (Abstr.)

Striem, B. J., U. Pace, U. Zehavi, M. Naim, and D. Lancet. 1989. Sweet tastants stimulate adenylate cyclase coupled to GTP-binding protein in rat tongue membranes. *Biochemical Journal.* 260:121–126.

Tang, C.-M., F. Presser, and M. Morad. 1988. Amiloride selectively blocks the low threshold (T) calcium channel. *Science.* 240:213–215.

Teeter, J. H., K. Sugimoto, and J. G. Brand. 1989. Ionic currents in taste cells and reconstituted taste epithelial membranes. *In* Chemical Senses: Molecular Aspects of Taste and Odor Reception. Vol. 1. J. G. Brand, J. H. Teeter, R. H. Cagan, and M. R. Kare, editors. Marcel Dekker, Inc., New York. 151–170.

Tonosaki, K., and M. Funakoshi. 1984. Effect of polarization of mouse taste cells. *Chemical Senses.* 9:381–387.

Tonosaki, K., and M. Funakoshi. 1988. Cyclic nucleotides may mediate taste transduction. *Nature.* 331:354–356.

Ureña, J., J. López-López, C. González, and J. López-Barneo. 1989. Ionic currents in dispersed chemoreceptor cells of the mammalian carotid body. *Journal of General Physiology.* 93:979–999.